A Long-Term Congestion Management Framework Through Market Zone Configuration Considering Collusive Bidding in Joint Spot Markets

Xueshan Lin, *Student Member, IEEE*, Tao Huang, *Senior Member, IEEE*, Xin Liu, *Student Member, IEEE*, Ettore F. Bompard, and Beibei Wang, *Senior Member, IEEE*

***Abstract*—The zonal market (ZM) adopted in Europe, in contrast to the nodal market (NM), reconciles the inconsistency between physical networks and administrative management. However, the growing integration of renewable energy sources (RESs) has introduced zonal supply-demand imbalances that exacerbate congestion and the need to re-dispatch. Furthermore, different clearing mechanisms between the day-ahead and real-time markets provide further opportunities for collusive bidding, decreasing total social welfare (TSW). Thus, this paper is the first to propose a long-term congestion management (CM) framework through a market zone (MZ) configuration approach with CM assessment considering collusive bidding in the joint spot markets. More specifically, a topology-based location division (TLD) method is proposed to partition optimal MZs, ensuring the minimum number of MZs based on critical branches. Then, a bi-level evolutionary model is developed to analyze the collusive bidding of producers in the day-ahead and ancillary service markets. Finally, the established framework is applied to a 20-bus test and simplified European systems. Our simulation on the 20-bus system shows that compared with the initial ZM and NM, the congestion cost of the optimized ZM decreased by 90% and 33%, respectively, while the TSW increased by around 13% and 1%, respectively.**

***Index Terms*—Congestion management, market zone configuration, collusive bidding analysis, joint spot markets, conventional generators, RESs.**

NOMENCLATURE

Abbreviations

ACT	Available transfer capacity.
ASM	Affinity score matrix.
CB	Critical branch.
CG/RES	Conventional generators/Renewable energy resource.
CM	Congestion management.
DA/AS	Day-ahead/Ancillary service.
FBMC	Flow-based market coupling.
ISF	Injection shift factor.
MS	Merchandise surplus.
MZ/ZM	Market zone/Zonal market.
NM	Nodal market.
PaB	Pay-as-bid.
PTDF	Power transfer distribution factor.
RAM	Remaining available margin.
RC	Re-dispatch cost.
SW/TSW	Social welfare/ Total social welfare.
TLD	Topology-based location division.
ZP/NP	Zonal price/ Nodal price.

Variables

$a_{\rm gc}/b_{\rm gc}$	Cost parameters of the g-th CG.
$a_{\rm l}/b_{\rm l}$	Utility parameters of the l-th demand.
$a_{\rm rc}$	Cost parameters of the r-th RES.
$a_{\rm d,g,t}/b_{\rm d,g,t}$	Strategic behavior of the g-th CG at time t in the DA market.
$a_{\rm r,g,t}$	Strategic behavior of the g-th CG at time t in the AS market.
$a_{\rm d,r,t}$	Strategic behavior of the r-th RES at time t in the DA market.
$a_{\rm r,r,t}$	Strategic behavior of the r-th RES at time t in the AS market.
$p_{\rm d,g,t}/p_{\rm d,r,t}$	Power output of the g-th CG/ r-th RES at time t in the DA market.
$d_{\rm d,l,t}$	Power consumption of the l-th load at time t in the DA market.
$\zeta_{\rm d}/\gamma_{\rm d}/\mu_{\rm d}$	Lagrange multiplier in the DA market.
$F_{\rm cmax}$	Power flow constraints of the c-th CB.
$p_{\rm gmin/max,t}$	Power output constraints of the g-th CG at time t.
$p_{\rm rmin/max,t}$	Power output constraints of the r-th RES at time t.
$d_{\rm lmin/max,t}$	Load consumption constraints of the l-th load at time t.
$ISF_{\rm c,z}$	c-by-z matrix with injection shift factor in the DA market.
${\rm GSK_{g/r/l}}^{\rm z}$	0-1 matrix with participants' connection location in the DA market.
$p_{\rm r,g,t}/p_{\rm r,r,t}$	Power output of the g-th CG/ r-th RES at time t in the AS market.

Manuscript received 21 July 2023; revised 25 December 2023 and 18 March 2024; accepted 19 April 2024. Date of publication 24 April 2024; date of current version 27 December 2024. This work was supported by the 2021 Humanities and Social Sciences Fund of the Ministry of Education of China "Research on In-Depth Mining Method of Power Data Value for Multi-scenario Social and Economic Development Evaluation" under Grant 21YJAZH083. Paper no. TPWRS-01144-2023. *(Corresponding author: Beibei Wang.)*

Xueshan Lin, Xin Liu, and Beibei Wang are with the School of Electrical Engineering, Southeast University, Nanjing 210096, China (e-mail: LXS_Christal@163.com; lxin@seu.edu.cn; wangbeibei@seu.edu.cn).

Tao Huang and Ettore F. Bompard are with the Dipartimento Energia, Politecnico di Torino, 10129 Turin, Italy (e-mail: tao.huang@polito.it; ettore.bompard@polito.it).

Color versions of one or more figures in this article are available at https://doi.org/10.1109/TPWRS.2024.3392934.

Digital Object Identifier 10.1109/TPWRS.2024.3392934

0885-8950 © 2024 IEEE. Personal use is permitted, but republication/redistribution requires IEEE permission.
See https://www.ieee.org/publications/rights/index.html for more information.

Authorized licensed use limited to: VinUni. Downloaded on January 23,2026 at 07:47:23 UTC from IEEE Xplore. Restrictions apply.

$d_{\mathrm{r,l,t}}$	Power consumption of the *l*-th load at time *t* in the AS market.
κ	RES forecast credibility.
$p_{r\max,t}^{forecast}$	Forecast value of RES output.
$\zeta_{\mathrm{r}}/\gamma_{\mathrm{r}}/\mu_{\mathrm{r}}$	Lagrange multiplier in the AS market.
F_{mmax}	Power flow constraints of the *m*-th branch.
$ISF_{\mathrm{m,n}}$	*m*-by-*n* matrix with injection shift factor in the AS market.
$\mathrm{GSK}_{\mathrm{g/r/l}}{}^{\mathrm{n}}$	0-1 matrix participants' connection location in the AS market.
$\lambda_{\mathrm{z,t}}$	ZP at time *t* in the DA market.

I. Introduction

A. Background and Motivations

WITH the increasing connection of renewable energy resources (RESs) and flexible demand, congestion is becoming more severe [1], [2]. The congestion there states a condition in which the power flow of some transmission lines/corridors in an electrical power grid can reach (more than) 100% of the capacity of the lines/corridors according to the market clearing results (the concept is closer to the definition of market congestion in [3]). The strategic behavior, is the participants adopt non-marginal price/non-marginal benefit quotations to gain more profit/benefit. Also, the recurring congestion problem in turn promotes strategic behavior and unreasonable incentives for market participants in electricity spot markets. In response, the Agency for Cooperation of Energy Regulators called for an effective zonal market (ZM) design, promoting fair transactions in the pan-European day-ahead (DA) electricity market and enhancing market efficiency [4].

To better understand and address the aforementioned issues, it is necessary to clarify three definitions: 1) What is long-term congestion management? 2) The impact of long-term congestion on the strategic behavior of generators, and 3) Why it is necessary to undertake long-term congestion management through market zone (MZ) configuration. For the first definition, even though congestion must be resolved hour by hour or 15 minutes by 15 minutes depending on the market regulation, according to different criteria and focus, congestion management can be long-term (i.e., the result can affect the resolution of congestion for quite a long term, e.g., several months or years) or short-term (the result can only affect for a short-term, e.g., a 15-minutes or one hour), can be physical (e.g., FACTS devices control [5], re-dispatch of the market results [6], etc. for short-term, transmission expansion [7] for long-term) or financial (transmission right) [8], can be capacity allocation (zonal marginal pricing [9], locational marginal pricing [10], the physical transmission right [11], etc.) or operational alleviation (load curtailment [12], counter trading [13], etc.), can be implicit (zonal marginal pricing [9], locational marginal pricing [10], etc.) or explicit (Fist-Come First Serviced [14], Pro-Rata [15], the physical transmission right [11], etc.). Thus, a solution for congestion management should usually be designed depending on the application scenarios and other market settings. For the second definition, the producers may exploit or induce congestion through strategic behaviors to gain additional profits. Long-term congestion is more likely to incentivize strategic behavior among market participants in the spot markets. For the third definition, the MZ configuration approach capitalizes on the foundational principles of the European existing market policies. It does not require the modification of other already established market regulations, such as trading schemes, commodities, relevant markets, short-term congestion management practices, etc.

In our paper, the proposed congestion management scheme is targeted as a long-term solution by configuring the MZ while not providing extra possibilities for market participants to execute market power.

B. Literature Review

This paper builds on three related areas: 1) CM; 2) MZ configuration approaches; 3) Strategic behavior analysis in ZM.

1) CM: With the increasing flexible demand and the growing volatility caused by the integration of RESs [16], congestion issues are becoming increasingly severe in electricity networks [17]. The solutions primarily involve technical adjustments and market regulation [18]. As mentioned before, technical adjustments include reactive power control [5], network reinforcement [7], load curtailment [12], Fist-Come First Serviced [14], Pro-Rata [15], network configuration [19], etc. Market regulation methods include market power mitigation, re-dispatch market [6], transmission right [8], [11], zonal marginal pricing [9], locational marginal pricing [10], counter trading [13], and other flexibility markets [20]. However, these approaches don't consider the mutual influence between the different original reasons for the congestion problem. Short-term congestion is triggered by strategic behavior in extreme scenarios or unforeseen events such as equipment failures or severe weather. Long-term congestion is caused by unreasonable grid structure or market configuration defects.

According to existing practices in European markets, wholesale market clearing is based on MZ configuration with relaxed intra-zonal grid constraints. Considering it contains the probability of changes in grid structure and reduces arbitrage opportunities of market participants, the market can operate in a way that decreases congestion caused by different reasons in the spot market clearing [21]. Thus, a practical approach for long-term CM through MZ configuration and depressing the strategic behaviors that trigger short-term congestion is crucially needed.

2) MZ Configuration Approaches: The approaches of MZ configuration can be divided into artificial intelligence and economics [22]. [23] presents an overview of clustering algorithms to configure MZs. [24], [25] clusters the network bus into zones using predefined features, objectives, and constraints. [26] clustering the MZs through a hierarchical clustering algorithm. The different mechanisms of nodal market (NM) clearing and ZM clearing can alter the strategic behavior of market participants. The artificial intelligence methods mainly rely on NM information, but ignore the flexible change of participants and a lack of result feedback, thereby affecting transmission congestion and leading to efficiency loss. The economics based on the physical indicator-based algorithms considers the effect on the performance of the Available Transfer Capacity (ATC) and the Flow-based market coupling (FBMC) model. It configures the ZM according to the market clearing result [27],

Authorized licensed use limited to: VinUni. Downloaded on January 23,2026 at 07:47:23 UTC from IEEE Xplore. Restrictions apply.

[28]. The flow limits between different zones in the ATC model depend on the pre-defined value given by system operators [29], providing rather inter-zonal financial constraints than physical constraints [30]. The omission of internal congestion leads to an unpredictable power flow [31]. Even though, practically, the MZ configuration is mainly driven by geographies, political forces, and then, after that, by the criticality of the transmission lines, most studies discuss MZ configuration mainly from the critical branches (CBs) point of view. Thus, the FBMC model was proposed to consider the power flow limits of CBs [32]. Conventionally, the CBs are selected based on two criteria: 1) the branch flow overpass 70% of its transmission capacity, and 2) the Power Transfer Distribution Factor (PTDF) of a branch is higher than a predefined threshold [33]. [34] calculate the CM through RC, and indicate that the re-defined CBs should be based on the expected congestion patterns. [9] and [35] investigated various approaches to alleviate congestion in ZM, including line constraint relaxation, outage situation assessment, and cross-border CM.

However, these approaches did not consider the collusive bidding of participants, leading to discrepancies between actual and estimated power flows [36], [37]. Also, it is difficult to find the optimal number of zones due to the complex interactions of the market. So, the optimal MZs should satisfy the pre-defined goal and the minimization number based on CBs.

3) Strategic Behavior Analysis: [38] research on the strategic behavior, which contains the location and price of producers in a ZM. [39] studies the electricity market power during COVID-19 in Italy to illustrate the relationship between congestion and strategic behavior. They do not propose a market power mitigation approach but only call for more pro-competitive action by the regulatory authority and pay more attention to strategic behaviors. A few ways exist to mitigate strategic behavior, which can be divided into five catalogs in practice and contain the divestiture of generation resources, contracts for must-run generators, forward contracts, reference prices, and financial penalties. All the above-listed mitigation methods are not a *free-market* outcome, i.e., these methods modified the market results. Of course, each of them has a specific scheme and applicable situation. Therefore, the strategic behavior mitigation must be matched with the market design and regulations (MZ configuration) to reduce the impact on the market outcome.

In our mind, different MZ configurations have different effects on market operation. [40], [41] shows the importance of considering the behavior of RES before MZ configuration. [42] mentioned that the highly imbalanced zonal prices caused by congestion may provide negative incentives to consumers, posing risks to system security. Therefore, the influence of the strategic behavior of participants on market congestion and operation status must be considered as a feedback mechanism in the MZ configuration. [43] analyzes the strategic behavior of energy storage systems in ZM, but does not provide the MZ configuration approach that considers strategic behavior and social welfare (SW). [44] discuss the coupling of dispatch and re-dispatch markets, and design the MZs with the aim of re-dispatch cost minimization. However, it only contains a single type of participant without considering market efficiency (or SW).

In the European electricity spot market, ZM clearing is implemented in the DA market, while the pay-as-bid (PaB) mechanism is used in the AS market [45], [46]. In the AS market, market participants can freely submit and execute bids, providing more substantial incentives to engage in collusive bidding. Therefore, accurate analysis of strategic behavior with considering market parameters, market structure, and market mechanisms is highly sought after.

Detailed comparison information (including advantages, disadvantages, and differences) of the existing approaches is presented in Table I. The proposed approach addresses the shortcomings of existing approaches by designing a long-term congestion management framework through market zone configuration considering collusive bidding in joint spot markets.

C. Contribution and Paper Organization

The main contributions of this study are as follows:

1) Proposed a congestion management scheme targeted for a long-term solution by adjusting the MZ configuration, while not providing an extra opportunity for market participants to execute market power, leading to an increased total social welfare (TSW).
2) A topology-based location division (TLD) method is proposed to minimize the number of zones based on CBs. This is essential to prevent the unreasonable increase in market zone numbers.
3) A bi-level analytical model is proposed to precisely estimate the collusive bidding of producers via a conjectured supply function game. The model considers the different market-clearing mechanisms of the DA and AS markets.
4) The proposed approach capitalizes on the foundational principles of the European existing market policies and does not require the modification of other already established market regulations.

The remainder of this paper is organized as follows. Section II presents the CM framework. Section III explains the MZ configuration approach, Section IV models the collusive bidding of producers in joint spot markets. Section V conducts a numerical simulation, and Section VI concludes the paper.

II. The Proposed Congestion Management Framework

A. Framework

The proposed CM framework mainly includes three mutually coupled parts: 1) selection of CBs, 2) partition of MZs (MZ configuration), and 3) collusive bidding modeling in joint spot markets (Fig. 1).

First, the MZ configuration is based on CBs. Then, inter-zonal clearing is performed based on MZs. If congestion is detected in the clearing results, re-dispatch adjustments are made. Due to the potential for cross-market collusion that arises from this multi-market clearing process, the possibility of collusive bidding needs to be considered. Finally, the outcomes of collusive bidding can further alter the existing CBs.

In particular, initial CBs are selected based on the remaining available margin (RAM) and PTDF [33]. Based on CBs, MZ

Authorized licensed use limited to: VinUni. Downloaded on January 23,2026 at 07:47:23 UTC from IEEE Xplore. Restrictions apply.

TABLE I
DETAILED COMPARISON INFORMATION OF THE EXISTING AND PROPOSED APPROACHES

Subject	Type	Difference	Advantage	Disadvantage	Reference
CM	Short-term	Include LMP/NP, market power mitigation, re-dispatch market, flexibility markets, etc.	To address the congestion issues caused by strategic behavior in extreme scenarios like equipment failures or severe weather	Ignore the mutual influence between the different original reasons for the congestion problem	[5], [6], [9], [10], [12], [13], [14], [15], [20]
	Long-term	Include reactive power control, network reinforcement, network configuration, etc.	To address the congestion problems arising from an impractical network structure and market configuration deficiencies		[7], [8], [11], [19]
MZ	Artificial Intelligence	Mainly rely on NM information through the clustering algorithms	Based on the accurate data, and aligns more closely with actual market operation	Ignore the flexible change of participants and result feedback, affecting transmission congestion and leading to efficiency loss	[23], [24], [25], [26]
	Economics	Configures the ZM according to the market clearing result	Theoretically analyze the congested transmission lines, which impact the market operation	Ignore the collusive bidding, leads to discrepancies between actual and estimated power flows	[27], [28], [29], [30], [31], [32], [33], [34], [35], [36], [37]
Strategic behavior	Single market	In the DA market	Simple calculation	Only a single type of participant or ignore the collusive bidding between different markets	[40], [41], [38], [39]
	DA and AS markets	In the DA and AS markets	Emphasizes the importance of MZ for SW and design the MZs with re-dispatch cost minimization	Only a single type of participant or ignore the influence of collusive bidding on TSW	[40], [41], [42], [43], [44]

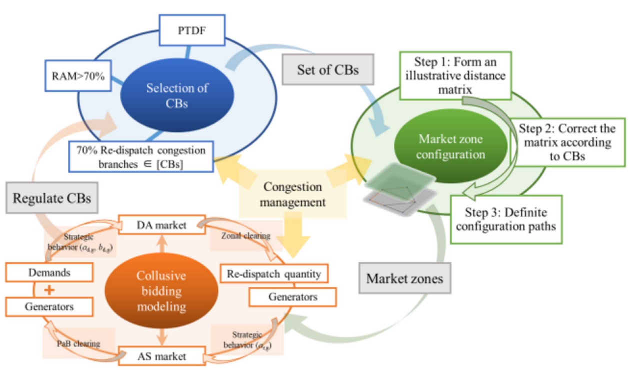

Fig. 1. The proposed CM framework.

can be defined through the proposed topology-based location division (TLD) method, which guarantees the minimum number of zones. With the defined MZs and CBs, collusive bidding involving CGs and RESs participating in the DA and AS markets is considered by a bi-level model under an evolutionary game. At the upper level, the producers maximize their own benefits via a conjectured supply function [47], [48] ($a_{\mathrm{d,g,t}}$, $b_{\mathrm{d,g,t}}$ in the DA market and $a_{\mathrm{r,g,t}}$ in the AS market). The lower level contains the DA and AS market clearing. The collusive bidding model is then analytically formulated through KKT conditions to accelerate the evolutionary process. DA market is cleared through social welfare maximization based on zonal price (ZP); while the objective of AS market clearing is RCs minimization with PaB. The results of collusive bidding lead to a new set of congested branches used to update CBs. The process continues until the termination criteria are reached, resulting in optimized MZs.

B. Algorithm

The proposed CM framework can be achieved with the following algorithm:

Algorithm 1: CM Approach.

Input:
(1) The parameters and topology of the electricity market
(2) Termination criteria: 70% re-dispatch congestion branches ∈ [CBs]
Output:
(1) The configured CBs and MZs

Step 1	Read the initial electricity market parameters ($p_{\mathrm{g/rmax,t}}$, $d_{\mathrm{lmax/min,t}}$, F_{cmax}, etc.) and the termination criteria
Step 2	Calculate PTDF and RAM and set the initial CBs
Step 3	Partition MZs according to the market configuration method (Topology-based Location Division (TLD)). Calculate the ZM parameters ($ISF_{\mathrm{c,z}}$, $\mathrm{GSK}^{\mathrm{z}}_{\mathrm{g/r/l}} = 0/1$)
Step 4	Initial re-dispatch quantity of load $d_{\mathrm{r,l,t}}$, and time period T
Step 5	For $h = 1$: H
Step 6	For $t = 1$: T
Step 7	Calculate the collusive bidding of producers ($a_{\mathrm{d,g,t}}$, $b_{\mathrm{d,g,t}}$, $a_{\mathrm{r,g,t}}$) by forecasting the supply function ((1)-(7))
Step 8	END For
Step 9	Calculate the market clearing results of producers' output, demand, and price in the DA and AS markets
Step 10	Get the re-dispatch congestion branches and TSW through the market-clearing results
Step 11	Calculate the percentage of re-dispatch congestion branches ∈ the set of CBs
Step 12	IF achieve the termination criteria, do
Step 13	$[CBs]_{\mathrm{configuration}} = [CBs]_{\mathrm{h}}$, $[Zones]_{\mathrm{configuration}} = [Zones]_{\mathrm{h}}$
Step 14	or
Step 15	$[CBs]_{\mathrm{h+1}} = [Re\text{-}dispatch\ congestion\ branches]$
Step 16	Return *Step 3*
Step 17	END For
Step 18	Output $[CBs]_{\mathrm{configuration}}$ and $[Zones]_{\mathrm{configuration}}$ as the optimized MZ configuration result

III. TLD BASED MARKET ZONE CONFIGURATION METHOD

ZM is used to simplify the market-clearing as closely as possible to pure economic clearing (generally referred to as market clearing without any network constraints. Thus, the market clearing only considers the bids/offers from the market participants to maximize the overall social surplus/welfare). A market zone should be determined to avoid high price differences

Authorized licensed use limited to: VinUni. Downloaded on January 23,2026 at 07:47:23 UTC from IEEE Xplore. Restrictions apply.

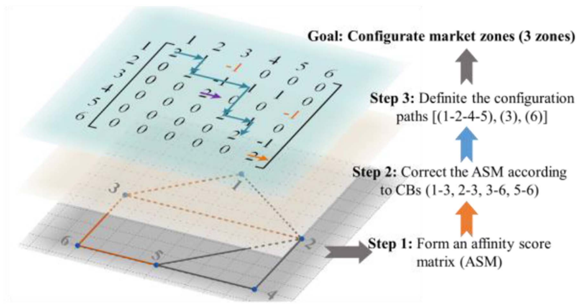

Fig. 2. The implementation process of the TLD approach.

among intra-zonal buses if we use the LMP model to calculate the price of each bus in the network. Thus, the number of zones should be determined only by substantial price differences. In cases where LMP-calculated price variances among buses within a zone are negligible, further partitioning that zone is unnecessary. On the other hand, CBs generally create high price differences on their terminals. Therefore, in this section, we propose the TLD method to optimally partition MZs, which can minimize the number of zones based on the CBs.

The specific implementation process is shown in Fig. 2.

As shown in Fig. 2(we use the 6-bus system as an example to illustrate the process), the first is to form an affinity score matrix (ASM). The ASM is an upper triangular matrix with rows and columns representing nodes. The element in the ASM is the assessment score of being in the same zone (2 means the zone will definitely be in the same zone, e.g., a node and itself; 1 means the nodes can be in the same zone, e.g., the terminals of a non-critical branch; 0 means unknown, e.g., not connected two nodes; -1 means the nodes definitely cannot be in the same zone, e.g., the terminals of CB).

Based on the ASM, the configuration search starts at node 1 and performs a horizontal search until 1 is reached, then switches to a vertical search until 2 has arrived. This search is repeated until the last column is reached. The inflection nodes (1 or 2) on the searched path form an MZ. The second search starts from the row of the first uncovered node. The process repeats until all the nodes are covered.

IV. Modeling of Collusive Bidding in Joint Markets

In this section, the strategic behavior of the producers is determined.

A. Mathematical Formulation

1) Modeling of Collusive Bidding in Joint Spot Markets: The Strategic behavior is analyzed through the bi-level model, the upper level involves the strategic behavior of producers with the aim of profit maximization in the DA and AS markets. Decision-makers assume that the bidding of other producers is known through the conjectured supply function. The lower level comprises DA and AS market clearing with the objective of social welfare maximization and system operating costs minimization, respectively. The bi-level model is not solved in a single step, instead, it iteratively derives equilibrium solutions for strategic behavior based on evolutionary game theory among the producers (CGs and RESs). The modeling of collusive bidding is illustrated in Fig. 3.

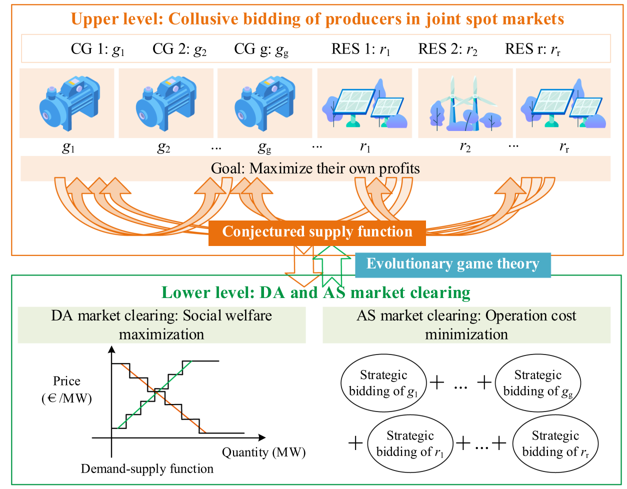

Fig. 3. Modeling of collusive bidding in joint spot markets.

2) Collusive Bidding of Producers in Joint Spot Markets: Each producer (owns one generator) in the upper level determines the offer function ($a_{\mathrm{d,g,t}}/a_{\mathrm{d,r,t}}$, $b_{\mathrm{d,g,t}}$ and $a_{\mathrm{r,g,t}}/a_{\mathrm{r,r,t}}$) in the DA and AS market to maximize their own profits. The strategic behavior of each producer (own CG/RES) are shown as (1a) and (1b), respectively.

$$
\begin{aligned}
& fg: \min \Big(\frac{a_{gc}}{2} p_{r,g,t}^2 + b_{gc} p_{r,g,t} - \lambda_{z,g,t}^* p_{d,g,t} \\
& \qquad - \frac{a_{r,g,t}}{2} (p_{r,g,t} - p_{d,g,t})^2 \Big) \\
& s.t. \\
& f1: DA\ market\ clearing\ optimization\ (2a) - (2f) \\
& f2: AS\ market\ clearing\ optimization\ (3a) - (3f) \\
& (g \in G, t \in T)
\end{aligned} \tag{1a}
$$

or

$$
\begin{aligned}
& fr: \min \left(a_{rc} \cdot p_{r,r,t}^* - \lambda_{z,r,t}^* p_{d,r,t}^* - a_{r,r,t} v_{r,r,t}^z \right) \\
& s.t. \\
& f1: DA\ market\ clearing\ optimization\ (2a) - (2f) \\
& f2: AS\ market\ clearing\ optimization\ (3a) - (3f) \\
& (r \in R, t \in T)
\end{aligned} \tag{1b}
$$

3) Model of DA and AS Market Clearing: In the DA market, the market clearing is modeled according to the actual operation process of the European market (Euphemia algorithm). The power exchange determines the g-th CG output ($g \in G$), r-th RES output ($r \in R$), and l-th load consumption ($l \in L$) at time t ($t \in T$) ($p_{\mathrm{d,g,t}}$ $p_{\mathrm{d,r,t}}$, and $d_{\mathrm{d,l,t}}$) through the optimization problem. If the power exchange accepts the offering price, the unit needs to be online to generate the cleared quantity; otherwise, it must

Authorized licensed use limited to: VinUni. Downloaded on January 23,2026 at 07:47:23 UTC from IEEE Xplore. Restrictions apply.

be shut down for the hours it is out-of-the-market (offers being rejected). The DA market adopts a double-sided auction model to maximize SW. Without loss of generality, a quadratic function is employed. The zonal price (ZP) is announced as $\lambda_{z,t}$, which can be calculated through the consist of Lagrange multiplier [ζ_t, $\gamma_{c,t}$, $\mu_{g/r/l,t}$] and the value of Injection Shift Factor (ISF) from zone z ($z \in Z$) to CB c ($c \in CB$) ($ISF_{c,z}$). Market clearing model can be calculated as follows:

$$f_1: \min \sum_{g\in G} \frac{a_{d,g,t}}{2} p_{d,g,t}^2 + b_{d,g,t}p_{d,g,t} + \sum_{r\in R} a_{d,r,t}p_{d,r,t} - \sum_{l\in L} \frac{a_l}{2} d_{d,l,t}^2 + b_l d_{d,l,t}, (t\in T) \tag{2a}$$

s.t.

$$\zeta_t \perp \left(\sum_{g\in G} p_{d,g,t} + \sum_{r\in R} p_{d,r,t} - \sum_{l\in L} d_{d,l,t} \right) = 0, t\in T \tag{2b}$$

$$\begin{cases} \gamma_{c,t}^- \perp \left(\sum_{z\in Z} ISF_{c,z} \left(\sum_{g\in G} p_{d,g,t} GSK_g^z \right.\right. \\ \left.\left. + \sum_{r\in R} p_{d,r,t} GSK_r^z - \sum_{l\in L} d_{d,l,t} GSK_l^z \right) - F_{c\max} \right) = 0 \\ \gamma_{c,t}^+ \perp \left(- \sum_{z\in Z} ISF_{c,z} \left(\sum_{g\in G} p_{d,g,t} GSK_g^z \right.\right. \\ \left.\left. + \sum_{r\in R} p_{d,r,t} GSK_r^z - \sum_{l\in L} d_{d,l,t} GSK_l^z \right) - F_{c\max} \right) = 0 \end{cases} \tag{2c}$$

$$\begin{cases} \mu_{g,t}^- \perp (p_{d,g,t} - p_{g\max,t}) = 0 \\ \mu_{g,t}^+ \perp (-p_{d,g,t}) = 0 \end{cases}, (g\in G, t\in T) \tag{2d}$$

$$\begin{cases} \mu_{r,t}^- \perp (p_{d,r,t} - p_{r\max,t}) = 0 \\ \mu_{r,t}^+ \perp (-p_{d,r,t}) = 0 \end{cases}, (r\in R, t\in T) \tag{2e}$$

$$\begin{cases} \mu_{l,t}^- \perp (d_{d,l,t} - d_{l\max,t}) = 0 \\ \mu_{l,t}^+ \perp (d_{l\min,t} - d_{d,l,t}) = 0 \end{cases}, (l\in L, t\in T) \tag{2f}$$

where, if *g*/*r*/*l* in zone *z*, $GSK_{g/r/l}^z = 1$. ISF matrix can be calculated through $ISF = B^{branch}(B^{bus})^{-1}$, the value is related to network topology. (2b) is the power balance constraint, and (2*c*) is the transmission constraint. (2d)–(2f) are the CGs, RESs power output, and demand consumption constraints, respectively. If it is necessary to consider the forecast uncertainty of RES, then let $p_{r\max,t} = \kappa p_{r\max,t}^{forecast}$, where κ is the RES forecast credibility, $p_{r\max,t}^{forecast}$ is the forecast value.

In the AS market, after collecting the bids, the producers are settled by the PaB mechanism to minimize the RC. Mathematically, the absolute value of RESs must be transformed by adding new variables $v_{r,r,t} = |p_{r,r,t} - p_{d,r,t}|$ to remove the sign [49].

$$f_2: \min \sum_{g\in G} \frac{a_{r,g,t}}{2} (p_{r,g,t} - p_{d,g,t})^2 + \sum_{r\in R} a_{r,r,t} v_{r,r,t}, (t\in T) \tag{3a}$$

s.t.

$$\varepsilon_t \perp \left(\sum_{g\in G} p_{r,g,t} + \sum_{r\in R} p_{r,r,t} - \sum_{l\in L} d_{r,l,t} \right) = 0, (t\in T) \tag{3b}$$

$$\begin{cases} \tau_{m,t}^- \perp \left(\sum_{n\in N} ISF_{m,n} \left(\sum_{g\in G} p_{r,g,t} GSK_g^n + \right.\right. \\ \left.\left. \sum_{r\in R} p_{r,r,t} GSK_r^n - \sum_{l\in L} d_{r,l,t} GSK_l^n \right) - F_{m\max} \right) = 0 \\ \tau_{m,t}^+ \perp \left(- \sum_{n\in N} ISF_{m,n} \left(\sum_{g\in G} p_{r,g,t} GSK_g^n + \right.\right. \\ \left.\left. \sum_{r\in R} p_{r,r,t} GSK_r^n - \sum_{l\in L} d_{r,l,t} GSK_l^n \right) - F_{m\max} \right) = 0 \\ (m\in M, t\in T) \end{cases} \tag{3c}$$

$$\begin{cases} \kappa_{r,t}^- \perp p_{r,r,t} - p_{d,r,t} - v_{r,r,t} = 0 \\ \kappa_{r,t}^+ \perp p_{d,r,t} - p_{r,r,t} - v_{r,r,t} = 0 \end{cases}, (r\in R, t\in T) \tag{3d}$$

$$\begin{cases} v_{g,t}^- \perp (p_{r,g,t} - p_{g\max,t}) = 0 \\ v_{g,t}^+ \perp (p_{g\min,t} - p_{r,g,t}) = 0 \end{cases}, (g\in G, t\in T) \tag{3e}$$

$$\begin{cases} v_{r,t}^- \perp (p_{r,r,t} - p_{r\max,t}) = 0 \\ v_{r,t}^+ \perp (p_{r\min,t} - p_{r,r,t}) = 0 \end{cases}, (r\in R, t\in T) \tag{3f}$$

Considering the required parameters, the relationship between the unknown variables $p_{d,r,t}{}^*, p_{d,r,t}{}^*, \zeta_t{}^*, \lambda_{z,t}{}^*$ and network parameters *ISF*, *GSK*, $NPG_{d,t}$, NPL_d in the DA market, the relationship between the unknown variables $p_{r,g,t}{}^*, p_{r,r,t}{}^*, v_{r,r,t}{}^*$ and the network parameters $NPG_{r,t}$, NPL_r, $d_{r,l,t}$ in the AS market can be calculated through KKT conditions. The process is in Appendix A (1) and the result is shown as follows. The DA and AS market clearing results are (4) and (5), respectively.

$$p_{d,g,t}^* = \begin{cases} \dfrac{\sum_{c\in CB} \gamma_{c,t}^{+*} ISF_{c,z} GSK_g^z - \sum_{c\in CB} \gamma_{c,t}^{-*} ISF_{c,z} GSK_g^z - \zeta_t^* - b_{d,g,t}^z + \mu_{g,t}^{+*} - \mu_{g,t}^{-*}}{a_{d,g,t}}, \mu_{g,t}^* = 0 \\ p_{g\max,t}, \mu_{g,t}^{-*} \neq 0 \\ 0, \mu_{g,t}^{+*} \neq 0 \\ (g\in G, t\in T) \end{cases} \tag{4a}$$

$$p_{d,r,t}^* = \begin{cases} p_{d,r,t}^*, \mu_{r,t}^* = 0 \\ pr\max, t, \mu_{r,t}^{-*} \neq 0 \\ 0, \mu_{r,t}^{+*} \neq 0 \end{cases}, (r\in R, t\in T) \tag{4b}$$

$$d_{d,l,t}^* = \begin{cases} \dfrac{\sum_{c\in CB} \gamma_{c,t}^{+*} ISF_{c,z} GSK_l^z - \zeta_t^* - \sum_{c\in CB} \gamma_{c,t}^{-*} ISF_{c,z} GSK_l^z - b_l^z + \mu_{l,t}^{-*} - \mu_{l,t}^{+*}}{a_l}, \mu_{l,t}^* = 0 \\ d_{l\max,t}, \mu_{l,t}^{-*} \neq 0 \\ d_{l\min,t}, \mu_{l,t}^{+*} \neq 0 \\ (l\in L, t\in T) \end{cases} \tag{4c}$$

$$\begin{cases} \zeta_t^* = \dfrac{NPG_{d,t} + \sum_{g\in G} \frac{\mu_{g,t}^{+*} - \mu_{g,t}^{-*}}{a_{d,g,t}} + \sum_{r\in R} p_{d,r,t}^* - NPL_d + \sum_{l\in L} \frac{\mu_{l,t}^{+*} - \mu_{l,t}^{-*}}{a_l}}{\sum_{g\in G} \frac{1}{a_{d,g,t}} - \sum_{l\in L} \frac{1}{a_l}} \\ \lambda_{z,t}^* = \sum_{c\in CB} \left(\gamma_{c,t}^+ ISF_{c,z} \right) - \sum_{c\in CB} \left(\gamma_{c,t}^- ISF_{c,z} \right) - \zeta_t^* \end{cases} \tag{4d}$$

Authorized licensed use limited to: VinUni. Downloaded on January 23,2026 at 07:47:23 UTC from IEEE Xplore. Restrictions apply.

$$\begin{cases} NPG_{d,t} = \sum_{g\in G} \frac{\sum_{c\in CB}\left(\gamma_{c,t}^{+*} ISF_{c,z} GSK_g^z - \gamma_{c,t}^{-*} ISF_{c,z} GSK_g^z\right)}{a_{d,g,t}} \\ \quad - \sum_{g\in G} \frac{b_{d,g,t}}{a_{d,g,t}} \\ NPL_d = \sum_{l\in L} \frac{\sum_{c\in CB}\left(\gamma_{c,t}^{+*} ISF_{c,z} - \gamma_{c,t}^{-*} ISF_{c,z}\right)}{a_l} + \sum_{l\in L} \frac{b_l}{a_l} \end{cases} \tag{4e}$$

$$p_{r,g,t}^* = \begin{cases} NPG_{r,t} + \frac{\upsilon_{g,t}^+ - \varepsilon_t^* - \upsilon_{g,t}^-}{a_{r,g,t}} + p_{d,g,t}^*, \upsilon_{g,t} = 0 \\ p_{g\max,t}, \upsilon_{g,t}^- \neq 0 \\ 0, \upsilon_{g,t}^+ \neq 0 \\ (t\in T, g\in G) \end{cases} \tag{5a}$$

$$p_{r,r,t}^* = \begin{cases} p_{r,r,t}^*, \upsilon_{r,t} = 0 \\ p_{r\max,t}, \upsilon_{r,t}^- \neq 0 \\ p_{r\min,t}, \upsilon_{r,t}^+ \neq 0 \end{cases}, (r\in R, t\in T) \tag{5b}$$

$$\varepsilon_t^* = \frac{\begin{array}{c}\sum_{r\in R} p_{r,r,t} + \sum_{g\in G} p_{d,g,t}^* + NPG_{r,t} \\ - \sum_{g\in G} \frac{\upsilon_{g,t}^- - \upsilon_{g,t}^+}{a_{r,g,t}} - \sum_{l\in L} d_{d,l,t}^* + d_{r,l,t}\end{array}}{\sum_{g\in G} \frac{1}{a_{r,g,t}}}, (t\in T) \tag{5c}$$

$$NPG_{r,t} = \sum_{g\in G} \frac{\begin{array}{c}\sum_{m\in M}\left(\tau_{m,t}^+ \sum_{n\in N} ISF_{m,n} GSK_g^n \right. \\ \left. - \tau_{m,t}^- \sum_{n\in N} ISF_{m,n} GSK_g^n\right)\end{array}}{a_{r,g,t}}, (t\in T) \tag{5d}$$

B. The Analytical Formulation of Collusive Bidding

Considering the (1) in the upper level and the clearing result (4) and (5) in the lower level of the model, the strategic coefficients of producers (own CG) to be determined can be concluded as (6) shown at the bottom of this page.

According to (4), (5), and (6), the collusive bidding of producers (own CG) in joint spot markets can be described in Appendix A (2) and the inequality constraints of market clearing can be converted by the *big-M* method [50], [51]. Then the strategic behavior of producers (own CG) can be calculated.

Furthermore, the marginal costs of RESs are often assumed to be a constant term and are always much lower than that of CGs. The strategic behavior of RES producers can be divided into 9 conditions in joint spot markets (Table II). Because of the low marginal cost of RES, the first two conditions in the DA and AS markets rarely occur in the real market. In addition, the third condition needs to be considered, which is determined by the network topology and parameters.

TABLE II
BIDDING BEHAVIOR OF RES PRODUCERS

	DA market			AS market		
Condition	$p_{d,r,t}^* = p_{r\max,t}$ $(\lambda_{z,t}^* > a_{d,r,t})$	$p_{d,r,t}^* = 0$ $(\lambda_{z,t}^* < a_{d,r,t})$	*Constraints* $(\lambda_{z,t}^* = a_{d,r,t})$	$p_{r,r,t}^* = p_{r\max,t}$ $(\upsilon_{r,t}^{-*} \neq 0)$	$p_{r,r,t}^* = 0$ $(\upsilon_{r,t}^{+*} \neq 0)$	*Constraints* $(\upsilon_{r,t}^* \neq 0)$
1	○			○		
2	○				○	
3	○					○
4		○		○		
5		○			○	
6		○				○
7			○	○		
8			○		○	
9			○			○

Different producers engage in a competitive process simulated by evolutionary game theory. Through iterations, the bi-level model yields collusive bidding strategies. In each iteration, producers determine their strategic behaviors using the conjectured supply function, assuming knowledge of other producers' strategic behaviors (e.g., the strategic behaviors of the g-th CG in the DA and AS markets are $a_{\mathrm{d,g,t}}$, $b_{\mathrm{d,g,t}}$, and $a_{\mathrm{r,g,t}}$; and strategic behaviors of the r-th RES in the DA and AS markets are $a_{\mathrm{d,r,t}}$ and $a_{\mathrm{r,r,t}}$). Initially, each producer assumes that the collusive bidding of other producers equals their cost.

In the process of iteration, the successful strategic offers can bring the producers extra profits due to the amount cleared; while the failed strategic offers get zero cleared quantities and zero profits. In the event of a strategy failure, our approach initiates the next iteration from the marginal price. If the marginal price remains unaccepted, the producer's cost is too high to clear, rendering the strategic behavior meaningless. In such cases, we define the offering curves of those producers as their marginal cost.

V. Numerical Simulation

To illustrate the proposed approach for congestion management through MZ configuration, we utilized a 20-bus system shown in Fig. 4. The parameters of the load and producers (data from GME in Italy [52]) are reported in Appendix B.

$$\begin{cases} \nabla f_g(a_{d,g,t}) = \left(1 - \frac{1}{a_{r,g,t}\sum_{g\in G}\frac{1}{a_{r,g,t}}}\right) \nabla p_{d,g,t}(a_{d,g,t})\left(a_{gc}p_{r,g,t} + b_{gc}\right) + \nabla\zeta_t(a_{d,g,t})p_{d,g,t} - \lambda_{z,g,t}\nabla p_{d,g,t}(a_{d,g,t}) \\ \quad + a_{r,g,t}(p_{r,g,t} - p_{d.g.t})\left(\frac{1}{a_{r,g,t}\sum_{g\in G}\frac{1}{a_{r,g,t}}}\right)\nabla p_{d,g,t}(a_{d,g,t}) = 0 \\ \nabla f_g(b_{d,g,t}) = \left(a_{gc}p_{r,g,t} + b_{gc}\right)\left(1 - \frac{1}{a_{r,g,t}\sum_{g\in G}\frac{1}{a_{r,g,t}}}\right)\nabla p_{d,g,t}(b_{d,g,t}) + \nabla\zeta_t(b_{d,g,t})p_{d,g,t} - \lambda_{z,g,t}\nabla p_{d,g,t}(b_{d,g,t}) \\ \quad + a_{r,g,t}(p_{r,g,t} - p_{d.g.t})\left(\frac{1}{a_{r,g,t}\sum_{g\in G}\frac{1}{a_{r,g,t}}}\right)\nabla p_{d,g,t}(b_{d,g,t}) = 0 \\ \nabla f_g(b_{r,g,t}) = a_{gc}p_{r,g,t}\nabla p_{r,g,t}(a_{r,g,t}) + b_{gc}\nabla p_{r,g,t}(a_{r,g,t}) - \frac{(p_{r,g,t} - p_{d,g,t})^2}{2} - a_{r,g,t}(p_{r,g,t} - p_{d,g,t})\nabla p_{r,g,t}(a_{r,g,t}) = 0 \\ (g\in G, t\in T) \end{cases} \tag{6}$$

Authorized licensed use limited to: VinUni. Downloaded on January 23,2026 at 07:47:23 UTC from IEEE Xplore. Restrictions apply.

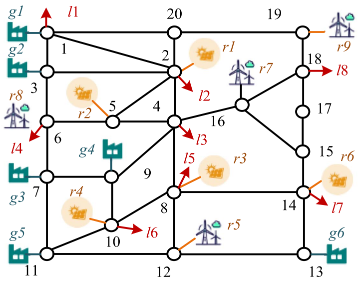

Fig. 4. 20-bus test system with 6 CGs and 9 RESs.

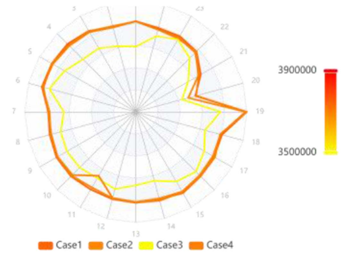

Fig. 5. The influence at the societal level in the joint spot markets: the TSW of the spot markets during 24 hours.

TABLE III
SETTINGS OF THE COMPARISON CASE

Case	Market type			Bidding behavior		Description
	NP	ZM_0	ZM_c	Collusion	Perfect	
1	○				○	Baseline
2	○			○		Comparison
3		○		○		Comparison
4			○	○		Proposed

(Baseline (*Case 1*): pure economic clearing in the DA market & perfect competition, *Case 4*: proposed approach, $ZM_{0/c}$: initial/configured ZM)

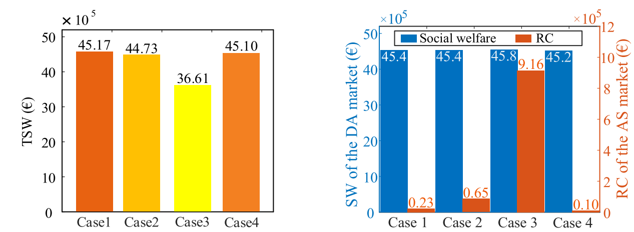

(a) TSW at $t = 19$ (b) SW and RC at $t = 19$

Fig. 6. The influence at the societal level in the joint spot markets: the separate details of TSW, SW, and RC at $t = 19$.

This section analyzes the proposed approach by

1) Comparing the market performance in the NM and ZM (*Case 1-Case 4*);
2) Comparing the collusive bidding in the NM and ZM (*Case 1-Case 4*);
3) Examining the impact of the consideration of different CBs and collusive bidding of MZ configuration process (*Case 3-Case 4*);
4) Comparing congestion in AS market through merchandise surplus (MS) (*Case 1-Case 4*);
5) Illustrating the impact of RES uncertainty;
6) Computational complexity in the extensive system.

All the results shown in the analysis hereinafter are weighted at the same hour to turn them into a 24-hour curve during one year. The data includes most of the possible variability in the RES power output and load demand, covering a daily variation and seasonal changes. The setting and description of the comparison cases is shown in Table III. The greater the proximity of the market configuration to Case 1, the more it approximates the concept of "Pure Economic Clearing and perfect competition", signifying that the partitioning of regional markets becomes more rational.

A. Market Performance

To illustrate the influence of the proposed approach at the societal level, the TSW is selected as the evaluation indicator in the joint spot markets. The differences in TSW among *Case 1-4* during 24 hours are shown in Fig. 5. The average TSW of *Case 1-4* during 24 hours are 3834600, 3782500, 3363200, and 3791100, respectively. Clearly, the proposed approach (*Case 4*) performs the best, which has the highest TSW considering the DA, AS, as well as strategic behaviors of all producers. In addition, by comparing *Case 2* and *Case 4*, *Case 2* has a significantly lower TSW, which implies a bad design of MZ can not only introduce more congestion but also provide more potential for gaming (collusive bidding in this case). The fact that the proposed method attains 98.87% of the TSW under perfect competition (*Case 1*) also shows that our proposed approach can greatly decrease the exercise of the collusive strategies of the producers and induct them to bid as close as under perfect competition.

To have more insight, we use a high-demand hour ($t = 19$) as an example, which would surely have a higher frequency of congestion. The TSW, SW, and RC are shown in Fig. 6.

The TSWs exhibit similar situations as the 24-hour TSW (Fig. 6(a)). However, it is clear that even though case 3 achieves the highest SW in DA by considering insufficient network constraints yet it causes a very high re-dispatch cost, leading to the lowest TSW (Fig. 6(b)). Instead, our proposed approach defines the best MZ configuration, which considers only a few most effective network constraints and does not shift the congestion-related cost to the AS. It shows that long-term congestion can be effectively managed by properly configured MZ, which will be changed for years.

Fig. 7 gives the market prices of all the cases for both the DA and AS markets. As in general RESs would be cleared at their highest offered quantity due to their low offering prices in the DA market; therefore, in all the cases, we only assume the bidding price for the decrease of RES units in the AS market as 5 euros/MWh (the green points in Fig. 7(a) and (b) are the locations of RES units). The upper layer in Fig. 7 represents the cleared PaB prices of various producers in the AS market, and the lower layer represents the NP/ZP in the DA market.

It is clear from Figs. 6(b), 7(a), and (b) that under the NP clearing scheme, both the SW and the NP are identical for *Case 1* and *Case 2*, which indicates that the collusive bidding strategy

Authorized licensed use limited to: VinUni. Downloaded on January 23,2026 at 07:47:23 UTC from IEEE Xplore. Restrictions apply.

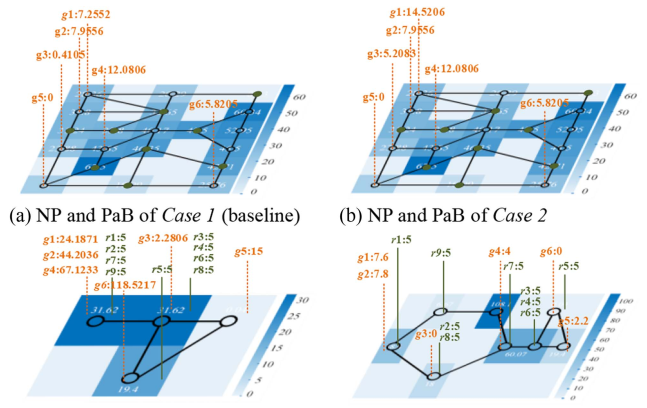

(a) NP and PaB of *Case 1* (baseline) (b) NP and PaB of *Case 2* (c) ZP and PaB of *Case 3* (d) ZP and PaB of *Case 4* (proposed approach)

Fig. 7. Price information of *Case1-4* in the DA and AS markets.

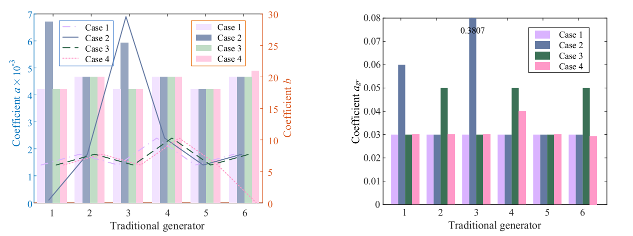

(a) Strategy in the DA market (b) Strategy in the AS market

Fig. 8. The collusive bidding in spot markets: the strategic behavior of CGs in the DA and AS markets.

of the producers requires them to offer their marginal cost to be cleared as much as possible in the DA market and create gaming potentials in the AS market. It can be observed by the RCs in Fig. 6(b) and the cleared PaB prices of g_1 and g_3 in Fig. 7(a) and (b).

For the ZP, Fig. 7(c) and (d) confirm the conclusion drawn by the previous comparison of TSWs. Even though the ZP for *Case 3* is much lower than that of *Case 4*, due to the lousy configuration of MZ in *Case 3*, producers can collusively increase the profit in the AS, leading to the lowest TSW. By contrast, our proposed approach (*Case 4*) has high ZP due to the successful identification of the CBs. Thus, it directly manages the congestion issue in the DA market at the cost of lowering a bit the SW in the DA market. However, thanks to the congestion in the DA market, the collusive bidding behaviors from producers are also suppressed; therefore, its RC is even lower than that of the perfect competition (*Case 1*).

B. Collusive Bidding

To further elaborate on the conclusion, the collusive bidding in spot markets is analyzed in Figs. 8–10.

In Fig. 8(a), the offering price of g_1 and g_3 increased significantly in *Case 2* compared to *Case 1*, but they are still slightly lower than that of the marginal generator. Therefore, the cleared quantities and revenues in the DA market are not changed (Fig. 9(a) and (b)). By contrast, the strategic offering prices in *Cases 3 & 4* in the DA market remain close to the perfect

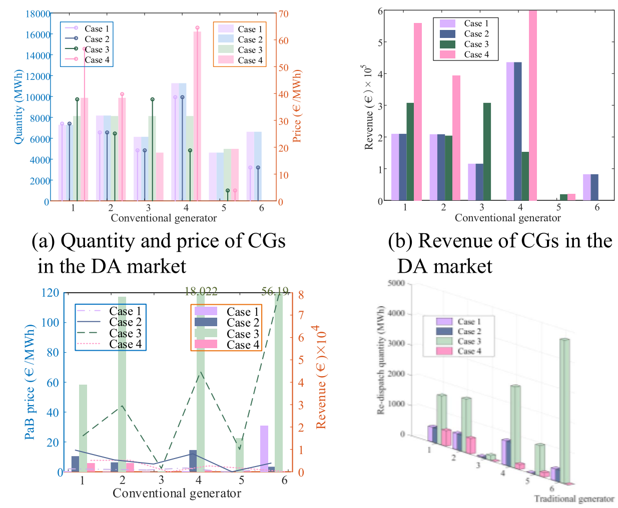

(a) Quantity and price of CGs in the DA market (b) Revenue of CGs in the DA market (c) Price and revenue of CGs in the AS market (d) Quantity of CGs in the AS market

Fig. 9. The collusive bidding in spot markets: the quantity, price, and revenue of CGs in the DA and AS market.

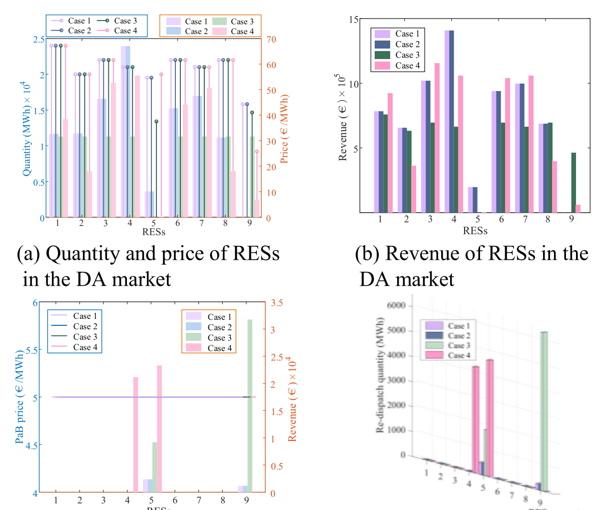

(a) Quantity and price of RESs in the DA market (b) Revenue of RESs in the DA market (c) Price and revenue of RESs in the AS market (d) Quantity of RESs in the AS market

Fig. 10. The collusive bidding in spot markets: the price, revenue, and quantity of CGs and RESs in the AS market.

competition level. However, the collusive bidding becomes clear if we look at the offering prices in the AS market. For example, in *Case 2*, g_1 and g_3 strategically increase their offering prices in the AS market to obtain higher revenue (Fig. 8(b)). However, as g_3 is expensive and is not in a critical location, its re-dispatched quantity equals 0 in the AS market (Fig. 9(c)); while the rest of the players can obtain higher revenue due to the increased demand (Fig. 9(c)).

In *Case 3*, among all 6 producers, g_2, g_4, and g_6 increase their offering prices (Fig. 8(b)) and obtain substantial excess revenues due to re-dispatch for congestion (Fig. 9(c)). By contrast, g_1, g_3, and g_5 keep their offering prices almost at the perfect competition level because they are not essential for solving congestion;

Authorized licensed use limited to: VinUni. Downloaded on January 23,2026 at 07:47:23 UTC from IEEE Xplore. Restrictions apply.

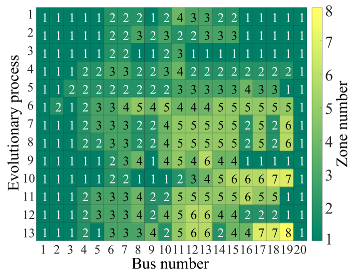

Fig. 11. The evolutionary process of MZ configuration: the process from initial to the optimized MZ configuration.

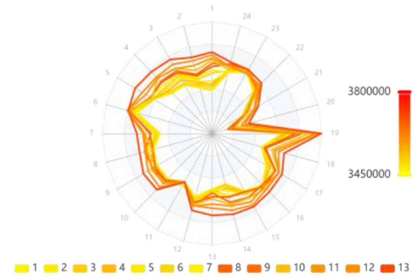

Fig. 12. The system performance of the evolutionary process of ZM configuration: the TSW (€) of the spot markets during 24 hours from evolution 1 (*Case 3*) to 13 (*Case 4*).

therefore, their revenues mainly come from increased demand in the AS market.

In *Case 4*, the strategic behaviors of all producers drastically decrease in the AS market (Fig. 8(b)). Only g_4 offers a slightly increased price, it is because no matter what MZ is, the system cannot completely avoid the congestion. It is also noticed that our proposed method sometimes can even achieve better re-dispatch results than the NP under perfect competition. The reason is that the NP under perfect competition obtains the optimal operational point by binding some line constraints, leading to a non-optimality when anything changes in the AS market. However, a better-configured MZ may still leave some margins for changes in the AS, leading to a possible lower re-dispatch amount.

In general, the producers located downstream of a congested line have locational advantages to increase their offering prices for higher profits strategically. However, during the iteration of our proposed method, if a producer indeed strategically grows its offer, the algorithm will reconfigure the MZ to introduce other producers to render the strategic offering effective. Therefore, the producers, even downstream of the congested lines, would offer to the market close to their marginal cost. When the entire iteration process stops, our proposed approach can thus identify all the CBs while mitigating the strategic behaviors simultaneously.

The situations for RESs are like those of the CGs; for the sake of space, we do not repeat the analysis again but summarize them in Fig. 10.

C. Market Zone Configuration

The evolutionary process of MZ configuration from the initial to the optimal MZ is shown in Fig. 11.

In Fig. 11, the process is undergoing 13 iterations. At the initial time, identifying congested branches leads to 4 market zones. With the precise selection of CBs, the optimal result is that the market can be divided into 8 MZs. The set of the congested branches in the AS market is ***con*** = [10], [12], [18], [21], [22], [24], [28], [30] and the set of CBs is ***cb*** = [6], [9], [10], [18], [21], [22], [28], [30]. The intersection of ***con*** ∩ ***cb*** accounts for 75% of the ***con***, which satisfies the termination condition. It should be noted that some elements in the ***cb*** are not in the ***con***, because listing them in the ***cb*** can avoid their presence in the AS market (e.g., branches 6 and 9).

Then, the impact of different CBs and bidding behaviors on system performance is analyzed in Fig. 12.

The evolutionary processes from 1 to 13 of market zone configuration represent the transition from *Case 3* (initial MZs) to *Case 4* (optimized MZs), and the innermost region corresponds to *Case 3*. In contrast, the outermost part corresponds to *Case 4*. In every process, the congested lines resulting from strategic behavior in different MZs will be adjusted as the CBs in the following process. The producers decide the collusive bidding based on the different MZs, leading to the other congestion lines. However, as the CBs that contribute to the collusive bidding are recognized, the overall market performance will improve, ultimately converging to optimal MZs. It is important to note that the efficacy of ZM cannot be solely determined by the number of MZs. For instance, in Process 7, despite having more MZs than 6, the TSW is lower in 7. Conversely, Process 4, with more MZs than 3, exhibits a higher TSW in 4. Therefore, the number of MZs does not necessarily correlate with improved or diminished market performance. Rather, it is the precision in identifying CBs and disregarding branches that facilitate collusive bidding, that improves market efficiency.

D. Congestion Management Assessment

The effectiveness of the long-term CM is assessed through the MS (calculated in the AS market) of *Case 1–Case 4*.

In Fig. 13(a), each case's magnitude represents the corresponding MS values at a specific time. For clarity, four subplots corresponding to the MS of *Cases 1–4* are given in Fig. 13(b)–(e). Our proposed method (*Case 4*) can significantly reduce the shadow prices of congested transmission branches in the AS market, even lower than the MS in the competitive market, due to effectively-identified CBs in the DA market. For example, at $t = 19$, $MS_{\text{case1}} = 1302000$, $MS_{\text{case2}} = 1428000$, $MS_{\text{case3}} = 9257800$, and $MS_{\text{case4}} = 935940$, which outperform the initial configuration by 889.14%, the NP-based collusive bidding market by 52.57%, and the NP-based competitive market by 39.11%.

E. Impact of RES Uncertainty

The impact of RES uncertainty on TSW is discussed through the change of κ, which represents the RES forecast credibility.

Authorized licensed use limited to: VinUni. Downloaded on January 23,2026 at 07:47:23 UTC from IEEE Xplore. Restrictions apply.

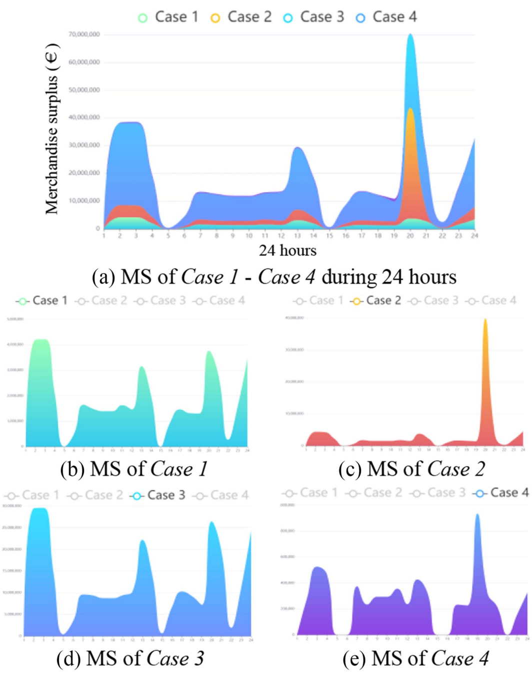

(a) MS of *Case 1* - *Case 4* during 24 hours

(b) MS of *Case 1* (c) MS of *Case 2*

(d) MS of *Case 3* (e) MS of *Case 4*

Fig. 13. The effectiveness of the long-term CM: the change of MS in the AS market between *Case 1* and *Case 4*.

TABLE IV
THE IMPACT OF RES UNCERTAINTY ON TSW

Case 4 compared with	98%	95%	93%	90%
Case 2	1.05%	1.56%	1.51%	1.64%
Case 3	14.85%	11.71%	21.54%	31.4%

In conclusion, the proposed approach performs relatively well under a certain level of RES prediction error.

TABLE V
THE COMPUTATIONAL COMPLEXITY OF THE PROPOSED APPROACH

Test system	Zone numbers	Configuration times/min
20-bus	8	3.1
Europe 240-bus	5	4.3
Europe 1354-bus	4	42.6

In conclusion, as shown in Table IV, the proposed approach performs relatively well under a certain level of RES prediction error.

F. Computational Complexity

Finally, the computational complexity of the proposed approach is shown in Table V and illustrated through several different scaled systems: the test 20-bus system, the simplified Europe 240-bus system, and the 1354-bus system.

The simulation is performed on 12th Gen Intel(R) Core (TM) i7-1260P, 2.10 GHz, 16G DDR4 ram, with Windows 11, MATLAB R2021b.

VI. CONCLUSION

This research primarily focuses on solving the long-term congestion problem and reducing the motivation of collusive bidding, which can decrease MS 8 times with initial MZs and guarantee the TSW in joint spot markets. It is worth noting that, considering data accuracy, we suggest that the configuration time for MZ should not exceed the known future network planning time.

However, this study analyzes the joint DA and AS markets without energy storage systems. To obtain more accurate results, the various types of participants need to be considered. Additionally, another kind of collusion exists among producers in the DA/ AS/ joint spot markets can be considered. Also, in practical engineering applications, many situations exceed the scope of this paper, such as political factors, the acceptance of the CBs' position, the congestion severity of the critical branches, etc. All of the elements can influence the MZ configuration results. We will consider the factors in the subsequent research to gradually refine the MZ configuration approach.

Therefore, to obtain more accurate results of MZ configuration, the model needs further improvement.

APPENDIX A

1) *DA and AS markets clearing:*

The Lagrange function and KKT conditions of DA market clearing can be concluded as:

$$
\begin{aligned}
L\left(p_{d,g,t}, p_{d,r,t}, d_{d,l,t}, \zeta_t\right) = &\sum_{g\in G} \frac{a_{d,g,t}}{2} p_{d,g,t}^2 + b_{d,g.t} p_{d,g,t} \\
&+ \sum_{r\in R} a_{d,r,t} p_{d,r.t} - \sum_{l\in L} \frac{a_l}{2} d_{d,l,t}^2 + b_l d_{d,l,t} \\
&+ \zeta_t \left(\sum_{g\in G} p_{d,g,t} + \sum_{r\in R} p_{d,r.t} - \sum_{l\in L} d_{d,l,t} \right) \\
&+ \sum_{c\in C} \gamma_{c,t}^{-} \left(\sum_{z\in Z} ISF_{c,z,t} \left(\sum_{g\in G} p_{d,g,t} GSK_g^z \right.\right. \\
&\left.\left. + \sum_{r\in R} p_{d,r.t} GSK_r^z - \sum_{l\in L} d_{d,l,t} GSK_l^z \right) - F_{c\max} \right) \\
&+ \sum_{c\in C} \gamma_{c,t}^{+} \perp \left(- \sum_{z\in Z} ISF_{c,z,t} \left(\sum_{g\in G} p_{d,g,t} GSK_g^z \right.\right. \\
&\left.\left. + \sum_{r\in R} p_{d,r.t} GSK_r^z - \sum_{l\in L} d_{d,l,t} GSK_l^z \right) - F_{c\max} \right) \\
&+ \sum_{g\in G} \mu_{g,t}^{-} \left(p_{d,g,t} - p_{g\max,t} \right) - \sum_{g\in G} \mu_{g,t}^{+} p_{d,g,t} \\
&+ \sum_{r\in R} \mu_{r,t}^{-} \left(p_{d,r.t} - p_{r\max,t} \right) + \sum_{r\in R} \mu_{r,t}^{+} \left(p_{r\min,t} - p_{d,r.t} \right) \\
&+ \sum_{l\in L} \mu_{l,t}^{-} \left(d_{d,l,t} - d_{l\max,t} \right) + \sum_{l\in L} \mu_{l,t}^{+} \left(d_{l\min,t} - d_{d,l,t} \right)
\end{aligned}
$$

Authorized licensed use limited to: VinUni. Downloaded on January 23,2026 at 07:47:23 UTC from IEEE Xplore. Restrictions apply.

$$\nabla f1\left(p_{d,g,t}\right)=a_{d,g,t}p_{d,g,t}+b_{d,g,t}+\zeta_t$$
$$+\sum_{c\in CB}\left(\gamma_{c,t}^{-}\sum_{z\in Z}ISF_{c,z,t}GSK_g^z\right)$$
$$-\sum_{c\in CB}\left(\gamma_{c,t}^{+}\sum_{z\in Z}ISF_{c,z,t}GSK_g^z\right)+\mu_{g,t}^{-}-\mu_{g,t}^{+}=0$$
$$\nabla f1\left(p_{d,r,t}\right)=a_{d,r,t}+\zeta_t+\sum_{c\in CB}\left(\gamma_{c,t}^{-}\sum_{z\in Z}ISF_{c,z,t}GSK_r^z\right)$$
$$-\sum_{c\in CB}\left(\gamma_{c,t}^{+}\sum_{z\in Z}ISF_{c,z,t}GSK_r^z\right)+\mu_{r,t}^{-}-\mu_{r,t}^{+}=0$$
$$\nabla f1\left(p_{d,l,t}\right)=-a_l d_{d,l,t}-b_l-\zeta_t$$
$$-\sum_{c\in CB}\left(\gamma_{c,t}^{-}\sum_{z\in Z}ISF_{c,z,t}GSK_l^z\right)$$
$$+\sum_{c\in CB}\left(\gamma_{c,t}^{+}\sum_{z\in Z}ISF_{c,z,t}GSK_l^z\right)+\mu_{l,t}^{-}-\mu_{l,t}^{+}=0$$
$$\nabla f1\left(\zeta_t\right)=\sum_{g\in G}p_{d,g,t}+\sum_{r\in R}p_{d,r,t}-\sum_{l\in L}d_{d,l,t}=0$$
$$\gamma_{c,t}^{-}\perp\sum_{z\in Z}ISF_{c,z,t}\left(\sum_{g\in G}p_{d,g,t}GSK_g^z+\sum_{r\in R}p_{d,r,t}GSK_r^z\right.$$
$$\left.-\sum_{l\in L}d_{d,l,t}GSK_l^z\right)-F_{c\max}=0$$
$$\gamma_{c,t}^{+}\perp-\sum_{z\in Z}ISF_{c,z,t}\left(\sum_{g\in G}p_{d,g,t}GSK_g^z+\sum_{r\in R}p_{d,r,t}GSK_r^z\right.$$
$$\left.-\sum_{l\in L}d_{d,l,t}GSK_l^z\right)-F_{c\max}=0$$
$$\mu_{g,t}^{-}\perp p_{d,g,t}-p_{g\max,t}=0$$
$$\mu_{g,t}^{+}\perp p_{d,g,t}-p_{g\min,t}=0$$
$$\mu_{r,t}^{-}\perp p_{d,r,t}-p_{r\max,t}=0$$
$$\mu_{r,t}^{+}\perp p_{d,r,t}-p_{r\min,t}=0$$
$$\mu_{l,t}^{-}\perp d_{d,l,t}-d_{l\max,t}=0$$
$$\mu_{l,t}^{+}\perp d_{l\min,t}-d_{d,l,t}=0$$

AS market clearing can be concluded as:

$$L\left(p_{r,g,t},p_{d,g,t},\upsilon_{r,r,t},\varepsilon_t\right)$$
$$=\sum_{g\in G}\frac{a_{r,g,t}}{2}\left(p_{r,g,t}-p_{d,g,t}\right)^2+\sum_{r\in R}a_{r,r,t}\upsilon_{r,r,t}$$
$$+\varepsilon_t\left(\sum_{g\in G}p_{r,g,t}+\sum_{r\in R}p_{r,r.t}-\sum_{l\in L}d_{r,l,t}\right)$$
$$+\sum_{m\in M}\tau_{m,t}^{-}\left(\sum_{z\in Z}ISF_{m,n,t}\left(\sum_{g\in G}p_{r,g,t}GSK_g^n\right.\right.$$
$$\left.\left.+\sum_{r\in R}p_{r,r.t}GSK_r^n-\sum_{l\in L}d_{r,l,t}GSK_l^n\right)-F_{m\max}\right)$$
$$+\sum_{c\in C}\tau_{m,t}^{+}\perp\left(-\sum_{z\in Z}ISF_{m,n,t}\left(\sum_{g\in G}p_{r,g,t}GSK_g^n\right.\right.$$
$$\left.\left.+\sum_{r\in R}p_{r,r,t}GSK_r^n-\sum_{l\in L}d_{d,l,t}GSK_l^n\right)-F_{m\max}\right)$$
$$+\sum_{r\in R}\kappa_{r,t}^{-}\left(p_{r,r,t}-p_{d,r,t}-\upsilon_{r,r,t}\right)$$
$$+\sum_{r\in R}\kappa_{r,t}^{+}\left(p_{d,r,t}-p_{r,r,t}-\upsilon_{r,r,t}\right)+\sum_{g\in G}\upsilon_{g,t}^{-}\left(p_{r,g,t}-p_{g\max,t}\right)$$
$$+\sum_{g\in G}\upsilon_{g,t}^{+}\left(p_{r,g,t}\right)+\sum_{r\in R}\upsilon_{r,t}^{-}\left(p_{r,r,t}-p_{r\max,t}\right)+\sum_{r\in R}\upsilon_{r,t}^{+}\left(p_{r,r,t}\right)$$
$$\nabla f2\left(p_{r,g,t}\right)=a_{r,g,t}\left(p_{r,g,t}-p_{d,g,t}\right)+\varepsilon_t$$
$$-\sum_{m\in M}\left(\tau_{m,t}^{+}\sum_{n\in N}ISF_{m,n,t}GSK_r^n\right.$$
$$\left.-\tau_{m,t}^{-}\sum_{n\in N}ISF_{m,n,t}GSK_r^n\right)+\upsilon_{g,t}^{-}-\upsilon_{g,t}^{+}=0$$
$$\nabla f2\left(p_{r,r,t}\right)=\varepsilon_t-\sum_{m\in M}\left(\tau_{m,t}^{+}\sum_{n\in N}ISF_{m,n,t}GSK_r^n\right.$$
$$\left.-\tau_{m,t}^{-}\sum_{n\in N}ISF_{m,n,t}GSK_r^n\right)+\kappa_{r,t}^{-}-\kappa_{r,t}^{+}+\upsilon_{r,t}^{-}-\upsilon_{r,t}^{+}=0$$
$$\nabla f2\left(\upsilon_{r,r,t}\right)=a_{r,r,t}-\kappa_{r,t}^{-}-\kappa_{r,t}^{+}=0$$
$$\nabla f2\left(\varepsilon_t\right)=\sum_{g\in G}p_{r,g,t}+\sum_{r\in R}p_{r,r,t}-\sum_{l\in L}d_{r,l,t}=0$$
$$\tau_{m,t}^{-}\perp\sum_{z\in Z}ISF_{c,z,t}\left(\sum_{g\in G}p_{d,g,t}GSK_g^z+\sum_{r\in R}p_{d,r,t}GSK_r^z\right.$$
$$\left.-\sum_{l\in L}d_{d,l,t}GSK_l^z\right)-F_{c\max}=0$$
$$\tau_{m,t}^{+}\perp-\sum_{z\in Z}ISF_{c,z,t}\left(\sum_{g\in G}p_{d,g,t}GSK_g^z+\sum_{r\in R}p_{d,r,t}GSK_r^z\right.$$

Authorized licensed use limited to: VinUni. Downloaded on January 23,2026 at 07:47:23 UTC from IEEE Xplore. Restrictions apply.

$$
\begin{aligned}
&- \sum_{l\in L} d_{d,l,t} GSK_l^z \Bigg) - F_{c\max} = 0\\
&\kappa_{r,t}^{-} \perp \left(p_{r,r,t} - p_{d,r,t} - \upsilon_{r,r,t}\right) = 0\\
&\kappa_{r,t}^{+} \perp \left(p_{d,r,t} - p_{r,r,t} - \upsilon_{r,r,t}\right) = 0\\
&\upsilon_{g,t}^{-} \perp \left(p_{r,g,t} - p_{g\max,t}\right) = 0\\
&\upsilon_{g,t}^{+} \perp \left(p_{r,g,t}\right) = 0\\
&\upsilon_{r,t}^{-} \perp \left(p_{r,r,t} - p_{r\max,t}\right) = 0\\
&\upsilon_{r,t}^{+} \perp p_{r,r,t} = 0
\end{aligned}
$$

2) Strategic behavior of producers

$$
\begin{cases}
p_{d,g,t}^{*} = \frac{\sum_{c\in CB}\left(\gamma_{c,t}^{+*} ISF_{c,z,t} - \gamma_{c,t}^{-*} ISF_{c,z,t}\right) - \zeta_{z,t}^{*} - b_{d,g,t} + \mu_{g,t}^{+*} - \mu_{g,t}^{-*}}{a_{d,g,t}}\\
\lambda_{z,t}^{*} = \sum_{c\in CB}\left(\gamma_{c,t}^{+} ISF_{c,z,t}\right) - \sum_{c\in CB}\left(\gamma_{c,t}^{-} ISF_{c,z,t}\right) - \zeta_{z,t}^{*}\\
\zeta_{z,t}^{*} = \frac{\begin{array}{c}\sum_{g\in G} \frac{\sum_{c\in CB}\left(\gamma_{c,t}^{+*} ISF_{c,z,t} - \gamma_{c,t}^{-*} ISF_{c,z,t}\right)}{a_{d,g,t}} - \sum_{g\in G}\frac{b_{d,g,t}}{a_{d,g,t}} + \sum_{g\in G}\frac{\mu_{g,t}^{+*} - \mu_{g,t}^{-*}}{a_{d,g,t}}\\ + \sum_{r\in R} p_{d,r,t}^{*} - \sum_{l\in L}\frac{\sum_{c\in CB}\left(\gamma_{c,t}^{+*} ISF_{c,z,t} - \gamma_{c,t}^{-*} ISF_{c,z,t}\right)}{a_l} + \sum_{l\in L}\frac{b_l}{a_l} - \sum_{l\in L}\frac{\mu_{l,t}^{-*} - \mu_{l,t}^{+*}}{a_l}\end{array}}{\sum_{g\in G}\frac{1}{a_{d,g,t}} - \sum_{l\in L}\frac{1}{a_l}}\\
p_{r,g,t}^{*} = \frac{-\varepsilon_t^{*} + \sum_{m\in M}\left(\tau_{m,t}^{+}\sum_{n\in N} ISF_{m,n,t} GSK_g^n - \tau_{m,t}^{-}\sum_{n\in N} ISF_{m,n,t} GSK_g^n\right) + \left(\upsilon_{g,t}^{+} - \upsilon_{g,t}^{-}\right)}{a_{r,g,t}} + p_{d,g,t}\\
\varepsilon_t^{*} = \frac{\sum_{r\in R} p_{r,r,t} + \sum_{g\in G} p_{d,g,t} + \sum_{g\in G}\frac{\sum_{m\in M}\left(\tau_{m,t}^{+}\sum_{n\in N} ISF_{m,n,t} GSK_g^n - \tau_{m,t}^{-}\sum_{n\in N} ISF_{m,n,t} GSK_g^n\right)}{a_{r,g,t}} + \sum_{g\in G}\frac{\upsilon_{g,t}^{+} - \upsilon_{g,t}^{-}}{a_{r,g,t}} - D_{r,t}}{\sum_{g\in G}\frac{1}{a_{r,g,t}}}
\end{cases}
$$

$$
\begin{cases}
\nabla f_g\left(a_{d,g,t}\right) = \left(a_{gc} p_{r,g,t} + b_{gc}\right)\left(1 - \frac{1}{a_{r,g,t}\sum_{g\in G}\frac{1}{a_{r,g,t}}}\right)\frac{\partial p_{d,g,t}}{\partial a_{d,g,t}} + \frac{\partial \zeta_t^{*}}{\partial a_{d,g,t}} p_{d,g,t} - \lambda_{g,z}^{*}\frac{\partial p_{d,g,t}}{\partial a_{d,g,t}} + \frac{\left(p_{r,g,t} - p_{d,g,t}\right)}{\sum_{g\in G}\frac{1}{a_{r,g,t}}}\frac{\partial p_{d,g,t}}{\partial a_{d,g,t}} = 0\\
\nabla \zeta_t^{*}\left(a_{d,g,t}\right) = \frac{p_{d,g,t} - \left(\mu_{g,t}^{+*} - \mu_{g,t}^{-*}\right) - \sum_{c\in CB}\left(\gamma_{c,t}^{+*} ISF_{c,z,t} - \gamma_{c,t}^{-*} ISF_{c,z,t}\right) + \zeta_t^{*}}{a_{d,g,t}^2\left(\sum_{g\in G}\frac{1}{a_{d,g,t}} - \sum_{l\in L}\frac{1}{a_l}\right)} = 0\\
\nabla p_{d,g,t}\left(a_{d,g,t}\right) = \frac{-\frac{\partial \zeta_t^{*}}{\partial a_{d,g,t}} a_{d,g,t} - \sum_{c\in CB}\left(\gamma_{c,t}^{+*} ISF_{c,z,t} - \gamma_{c,t}^{-*} ISF_{c,z,t}\right) + \zeta_t^{*} + b_{d,g,t} - \left(\mu_{g,t}^{+*} - \mu_{g,t}^{-*}\right)}{a_{d,g,t}^2} = 0\\
\nabla f_g\left(b_{d,g,t}\right) = \left(a_{gc} p_{r,g,t} + b_{gc}\right)\left(1 - \frac{1}{a_{r,g,t}\sum_{g\in G}\frac{1}{a_{r,g,t}}}\right)\left(\frac{1}{a_{d,g,t}^2\left(\sum_{g\in G}\frac{1}{a_{d,g,t}} - \sum_{l\in L}\frac{1}{a_l}\right)} - \frac{1}{a_{d,g,t}}\right)\\
\quad - \lambda_z^{*}\left(\frac{1}{a_{d,g,t}^2\left(\sum_{g\in G}\frac{1}{a_{d,g,t}} - \sum_{l\in L}\frac{1}{a_l}\right)} - \frac{1}{a_{d,g,t}}\right)\\
- \frac{1}{a_{d,g,t}\left(\sum_{g\in G}\frac{1}{a_{d,g,t}} - \sum_{l\in L}\frac{1}{a_l}\right)} p_{d,g,t} + \left(p_{r,g,t} - p_{d,g,t}\right)\left(\frac{1}{\sum_{g\in G}\frac{1}{a_{r,g,t}}}\right)\left(\frac{1}{a_{d,g,t}^2\left(\sum_{g\in G}\frac{1}{a_{d,g,t}} - \sum_{l\in L}\frac{1}{a_l}\right)} - \frac{1}{a_{d,g,t}}\right) = 0\\
\nabla f_g\left(a_{r,g,t}\right) = a_{gc} p_{r,g,t}\frac{\partial p_{r,g,t}}{\partial a_{r,g,t}} + b_{gc}\frac{\partial p_{r,g,t}}{\partial a_{r,g,t}} - \frac{\left(p_{r,g,t} - p_{d,g,t}\right)^2}{2} - a_{r,g,t}\left(p_{r,g,t} - p_{d,g,t}\right)\frac{\partial p_{r,g,t}}{\partial a_{r,g,t}} = 0\\
\nabla p_{r,g,t}\left(a_{r,g,t}\right) = \frac{-\frac{\partial \varepsilon_t^{*}}{\partial a_{r,g,t}} a_{r,g,t} + \varepsilon_t^{*} - \sum_{m\in M}\left(\tau_{m,t}^{+}\sum_{n\in N} ISF_{m,n,t} GSK_g^n - \tau_{m,t}^{-}\sum_{n\in N} ISF_{m,n,t} GSK_g^n\right) - \left(\upsilon_{g,t}^{+} - \upsilon_{g,t}^{-}\right)}{\left(a_{r,g,t}\right)^2} = 0\\
\nabla \varepsilon_t\left(a_{r,g,t}\right) = \frac{-\sum_{m\in M}\left(\tau_{m,t}^{+}\sum_{n\in N} ISF_{m,n,t} GSK_g^n - \tau_{m,t}^{-}\sum_{n\in N} ISF_{m,n,t} GSK_g^n\right) - \left(\upsilon_{g,t}^{+} - \upsilon_{g,t}^{-}\right)}{a_{r,g,t}^2\sum_{g\in G}\frac{1}{a_{r,g,t}}}\\
+ \frac{\sum_{r\in R} p_{r,r,t} + \sum_{g\in G} p_{d,g,t} + \sum_{g\in G}\frac{\sum_{m\in M}\left(\tau_{m,t}^{+}\sum_{n\in N} ISF_{m,n,t} GSK_g^n - \tau_{m,t}^{-}\sum_{n\in N} ISF_{m,n,t} GSK_g^n\right)}{a_{r,g,t}} + \sum_{g\in G}\frac{\upsilon_{g,t}^{+} - \upsilon_{g,t}^{-}}{a_{r,g,t}} - D_{r,t}}{\left(a_{r,g,t}\sum_{g\in G}\frac{1}{a_{r,g,t}}\right)^2} = 0
\end{cases}
$$

Authorized licensed use limited to: VinUni. Downloaded on January 23,2026 at 07:47:23 UTC from IEEE Xplore. Restrictions apply.

APPENDIX B

Type	Bus	b	a	$p_{\min}$	$p_{\max}$
CGs	1	18	0.0014	0	35000
	3	20	0.0018	0	30000
	7	18	0.0014	0	30000
	9	20	0.0024	0	35000
	11	18	0.0014	0	35000
	13	20	0.0018	0	30000
RESs	2	0.03	0	0	24000
	5	0.04	0	0	20000
	6	0.03	0	0	22000
	8	0.03	0	0	21000
	10	0.04	0	0	20000
	12	0.03	0	0	22000
	14	0.03	0	0	21000
	16	0.03	0	0	22000
	19	0.03	0	0	21000

REFERENCES

[1] M. Sarfati and M. R. Hesamzadeh, "Production efficiency of nodal and zonal pricing in imperfectly competitive electricity markets," *Energy Strategy Rev.*, vol. 24, pp. 193–206, Feb. 2019.

[2] S. Pearson, S. Wellnitz, and P. C. Granado, "The value of TSO-DSO coordination in re-dispatch with flexible decentralized energy sources: Insights for Germany in 2030," *Appl. Energy*, vol. 326, no. 15, Nov. 2022, Art. no. 119905.

[3] European Commission, "Commission Regulation (EU) 2015/1222 of 24 July 2015, establishing a guideline on capacity allocation and congestion management," *Off. J. Eur. Union*, vol. 197, pp. 24–72, Jul. 2015.

[4] ACER, "Report on the result of monitoring the margin available for cross-zonal electricity trade in the EU in the second semester of 2020," *ACER*, Ljubljana Slovenia, Jun. 2021. [Online]. Available: https://www.acer.europa.eu/sites/default/files/documents/Publications/ACER%20MACZT%20Report%202021.pdf

[5] S. H. Dolatabadi, M. Ghorbanian, and P. Siano, and N. D. Hatziargyriou, "An enhanced IEEE 33 bus benchmark test system for distribution system studies," *IEEE Trans. Power Syst.*, vol. 36, no. 3, pp. 2565–2572, May 2021.

[6] S. Pearson, S. Wellnitz, and P. C. del Granado, "The value of TSO-DSO coordination in re-dispatch with flexible, decentralized energy sources: Insights for Germany in 2030," *Appl. Energy*, vol. 326, Nov. 2022, Art. no. 119905.

[7] A. S. Dagoumas and N. E. Koltsaklis, "Review of models for integrating renewable energy in the generation expansion planning," *Appl. Energy*, vol. 242, pp. 1573–1587, Mar. 2019.

[8] K. Zhang, S. Troitzsch, and S. Hani, "Coordinated market design for peer-to-peer energy trade and ancillary services in distribution grids," *IEEE Trans. smart grid*, vol. 11, no. 4, pp. 2929–2941, Jul. 2020.

[9] M. Ambrosius, V. Grimm, and T. Kleinert, "Endogenous price zones and investment incentives in electricity markets: An application of multilevel optimization with graph partitioning," *Energy Econ.*, vol. 92, Oct. 2020, Art. no. 104879.

[10] K. Zheng, Y. Wang, K. Liu, and Q. Chen, "Locational marginal price forecasting: A componential and ensemble approach," *IEEE Trans. Smart Grid*, vol. 11, no. 5, pp. 4555–4564, Sep. 2020.

[11] V. Sarkar and S. A. Khaparde, "A comprehensive assessment of the evolution of financial transmission rights," *IEEE Trans. Power Syst.*, vol. 23, no. 4, pp. 1783–1795, Nov. 2008.

[12] V. K. Prajapati and V. Mahajan, "Reliability assessment and congestion management of power system with energy storage system and uncertain renewable resources," *Energy*, vol. 215, Jan. 2021, Art. no. 119134.

[13] J. Dijk and B. Willems, "The effect of counter-trading on competition in electricity markets," *Energy Policy*, vol. 39, no. 3, pp. 1764–1773, Mar. 2011.

[14] E. Hasan and F. D. Galiana, "Electricity markets cleared by merit order—Part II: Strategic offers and market power," *IEEE Trans. Power Syst.*, vol. 23, no. 2, pp. 372–379, May 2008.

[15] A. J. Conejo, J. M. Arroyo, N. Alguacil, and A. L. Guijarro, "Transmission loss allocation: A comparison of different practical algorithms," *IEEE Trans. Power Syst.*, vol. 17, no. 3, pp. 571–576, Aug. 2002.

[16] S. Yang, K. W. Lao, Y. Chen, and H. Hui, "Resilient distributed control against false data injection attacks for demand response," *IEEE Trans. Power Syst., early access*, vol. 39, no. 2, pp. 2837–2853, Mar. 2024.

[17] IRENA, "Renewable capacity statistics 2020 International Renewable Energy Agency," Abu Dhabi, Oct. 2020. [Online]. Available: https://www.irena.org/-/media/Files/IRENA/Agency/Publication/2020/Mar/IRENA_RE_Capacity_Statistics_2020.pdf

[18] M. Attar, S. Repo, and P. Mann, "Congestion management market design approach for the Nordics and Central Europe," *Appl. Energy*, vol. 313, no. 1, May 2022, Art. no. 118905.

[19] Y. Weng, J. Xie, P. Wang, and H. D. Nguyen, "Asymmetrically reciprocal effects and congestion management in TSO-DSO coordination through feasibility regularizer," *IEEE Trans. Power Syst.*, vol. 38, no. 2, pp. 1948–1962, Mar. 2023.

[20] K. Chakravarthi, P. Bhui, N. K. Sharma, and B. C. Pal, "Real time congestion management using generation re-dispatch: Modeling and controller design," *IEEE Trans. Power Syst.*, vol. 38, no. 3, pp. 2189–2203, May 2023.

[21] H. Hobbie, J. Mehlem, and C. Wolff, "Impact of model parametrization and formulation on the explorative power of electricity network congestion management models-insights from a grid model comparison experiment," *Renewable Sustain. Energy Rev.*, vol. 159, May 2022, Art. no. 112163.

[22] L. Corona, A. Mochon, and Y. Saez, "Electricity market integration and impact of renewable energy sources in the Central Western Europe region: Evolution since the implementation of the flow-based market coupling mechanism," *Energy Rep.*, vol. 8, pp. 1768–1788, Nov. 2022.

[23] G. Chicco et al., "Overview of the clustering algorithms for the formation of the bidding zones," in *Proc. 54th Int. Universities Power Eng. Conf.*, 2019 pp. 1–6.

[24] P. Colella, A. Mazza, and E. Bompard, "Model-based identification of alternative bidding zones: Applications of clustering algorithms with topology constraints," *Energies*, vol. 14, no. 10, May 2021, Art. no. 2763.

[25] M. Kittel, H. Hobbie, and C. Dierstein, "Temporal aggregation of time series to identify typical hourly electricity system states: A systematic assessment of relevant cluster algorithms," *Energy*, vol. 247, no. 15, May 2022, Art. no. 123458.

[26] L. Michi, F. Quaglia, and E. Bompard, "Optimal bidding zone configuration: Investigation on model-based algorithms and their application to the Italian power system," in *Proc. Int. Annu. Conf.*, 2019 pp. 1–6.

[27] D. Schönheit, K. Bruninx, and M. Kenis M, "Improved selection of critical network elements for flow-based market coupling based on congestion patterns," *Appl. Energy*, vol. 247, no. 15, May 2022, Art. no. 123458.

[28] M. Bjørndal and E. Bjørndal, "Pricing and congestion management in coupled European wholesale markets," Energy Lab/ENE Kristian Gerhard Jebsen Centre NHH, Bergen Norwegian, Sep. 2017. [Online]. Available: https://www.uib.no/sites/w3.uib.no/files/attachments/mette_bjorndal.pdf

[29] R. Weinhold and R. Mieth, "Uncertainty-aware capacity allocation in flow-based market coupling," *IEEE Trans. Power Syst.*, vol. 39, no. 1, pp. 147–159, Jan. 2024.

[30] M. Attar, S. Repo, and P. Mann, "Congestion management market design-approach for the Nordics and Central Europe," *Appl. Energy*, vol. 313, no. 1, May 2022, Art. no. 118905.

[31] T. Kristiansen, "The flow-based market coupling arrangement in Europe: Implications for traders," *Energy Strategy Rev.*, vol. 27, Jan. 2020, Art. no. 100444.

[32] T. Huang, E. Bompard, and Z. Yan, "Congestion management impacts on bilateral electricity markets under strategic negotiation," *Electric power Syst. Res.*, vol. 81, no. 5, pp. 1161–1170, May 2011.

[33] Z. Bashir and T. François, "Supervised learning-assisted modeling of flow-based domains in European resource adequacy assessments," *Appl. Energy*, vol. 325, no. 1, Nov. 2022, Art. no. 119875.

[34] I. A. Puiu and R. A. Hauser, "Principled data completion of network constraints for day ahead auctions in power markets," *IEEE Trans. Power Syst.*, vol. 37, no. 6, pp. 4460–4472, Nov. 2022.

[35] H. Hobbie, J. Mehlem, and C. Wolff, "Impact of model parametrization and formulation on the explorative power of electricity network congestion management models-insights from a grid model comparison experiment," *Renewable Sustain. Energy Rev.*, vol. 159, May 2022, Art. no. 112163.

[36] P. Razmi, M. O. Buygi, and M. Esmalifalak, "A machine learning approach for collusion detection in electricity markets based on Nash equilibrium theory," *J. Modern Power Syst. Clean Energy*, vol. 9, no. 1, pp. 170–180, Jan. 2021.

[37] X. Lei, T. Huang, and Y. Yang, "A bi-layer multi-time coordination method for optimal generation and reserve schedule and dispatch of a grid-connected microgrid," *IEEE Access*, vol. 7, pp. 44010–44020, Feb. 2019.

Authorized licensed use limited to: VinUni. Downloaded on January 23,2026 at 07:47:23 UTC from IEEE Xplore. Restrictions apply.

[38] A. Eicke, "Where should generators be built in a zonal electricity market? A numerical analysis of administratively determined investment signals," ZBW—Leibniz Information Centre for Economics, Kiel Hamburg, Sep. 2022. [Online]. Available: https://www.econstor.eu/handle/10419/261346

[39] S. Bigerna, C. A. Bollino, and M. C. D'Errico, "COVID-19 lockdown and market power in the Italian electricity market," *Energy Policy*, vol. 161, Feb. 2022, Art. no. 112700.

[40] E. S. Fianu, D. F. Ahelegbey, and L. Grossi L, "Modeling risk contagion in the Italian zonal electricity market," *Eur. J. Oper. Res.*, vol. 298, no. 2, pp. 656–679, Apr. 2022.

[41] K. Chakravarthi, P. Bhui, N. K. Sharma, and B. C. Pal, "Real-time congestion management using generation re-dispatch: Modeling and controller design," *IEEE Trans. Power Syst.*, vol. 38, no. 3, pp. 2189–2203, May 2023.

[42] A. Eicke and T. Schittekatte, "Fighting the wrong battle? A critical assessment of arguments against nodal electricity prices in the European debate," *Energy Policy*, vol. 170, Nov. 2022, Art. no. 113220.

[43] E. Bjørndal, M. H. Bjørndal, and S. Coniglio, "Energy storage operation and electricity market design: On the market power of monopolistic storage operators," *Eur. J. Oper. Res.*, vol. 307, no. 2, pp. 887–909, Jun. 2023.

[44] K. Poplavskaya, G. Totschnig, and F. Leimgruber, "Integration of day-ahead market and re-dispatch to increase cross-border exchanges in the European electricity market," *Appl. Energy*, vol. 278, no. 15, Nov. 2020, Art. no. 115669.

[45] N. Stevens and A. Papavasiliou, "Application of the level method for computing locational convex hull prices," *IEEE Trans. Power Syst.*, vol. 37, no. 5, pp. 3958–3968, Sep. 2022.

[46] I. Pavić, H. Pandžić, and T. Capuder, "Electric vehicle aggregator as an automatic reserves provider under uncertain balancing energy procurement," *IEEE Trans. Power Syst.*, vol. 38, no. 1, pp. 396–410, Jan. 2023.

[47] C. J. Day, B. F. Hobbs, and J. S. Pang, "Oligopolistic competition in power networks: A conjectured supply function approach," *IEEE Trans. power Syst.*, vol. 17, no. 3, pp. 597–607, Aug. 2002.

[48] W. Xian, L. Yuzeng, and Z. Shaohua, "Oligopolistic equilibrium analysis for electricity markets: A nonlinear complementarity approach," *IEEE Trans. Power Syst.*, vol. 19, no; no. 3, pp. 1348–1355, Aug. 2004.

[49] D. Berstsimas, *Introduction to Linear Optimization*. Belmont, MA, USA: Athena Scientific, 1997.

[50] S. González, F. Feijoo, F. Basso, V. Subramanian, S. Sankaranarayanan, and T. K. Das, "Routing and charging facility location for EVs under nodal pricing of electricity: A bilevel model solved using special ordered set," *IEEE Trans. Smart Grid*, vol. 13, no. 4, pp. 3059–3068, Jul. 2022.

[51] E. Prat and S. Chatzivasileiadis, "Learning active constraints to efficiently solve linear bilevel problems: Application to the generator strategic bidding problem," *IEEE Trans. Power Syst.*, vol. 38, no. 3, pp. 2376–2387, May 2023.

[52] Gestore Mercati energetic, "Electricity markets, results, and statistics," Report, 2022. [Online]. Available: https://www.mercatoelettrico.org/En/Tools/Accessodati.aspx?ReturnUrl=%2fEn%2fEsiti%2fMGP%2fEsitiMGP.aspx

Authorized licensed use limited to: VinUni. Downloaded on January 23,2026 at 07:47:23 UTC from IEEE Xplore. Restrictions apply.